Journal of Neurology (2022) 269:2715–2719
https://doi.org/10.1007/s00415-021-10869-z

ORIGINAL COMMUNICATION

Increased aneurysm wall permeability colocalized with low wall shear stress in unruptured saccular intracranial aneurysm

Yajie Wang[1] · Jie Sun[2] · Rui Li[1] · Peng Liu[3] · Xian Liu[1] · Jiansong Ji[4] · Chunmiao Chen[4] · Yu Chen[1] · Haikun Qi[5] · Yunduo Li[1] · Longhui Zhang[3] · Luqiong Jia[3] · Fei Peng[3] · Mingzhu Fu[1] · Yishi Wang[6] · Min Xu[4] · Chunli Kong[4] · Shuiwei Xia[4] · Xiaole Wang[1] · Le He[1] · Qiang Zhang[1] · Zhensen Chen[7] · Aihua Liu[3] · Youxiang Li[3] · Ming Lv[3] · Huijun Chen[1]

Received: 6 October 2021 / Revised: 19 October 2021 / Accepted: 20 October 2021 / Published online: 3 November 2021
© The Author(s), under exclusive licence to Springer-Verlag GmbH Germany 2021

Abstract

Aneurysm wall permeability has recently emerged as an in vivo marker of aneurysm wall remodeling. We sought to study the spatial relationship between hemodynamic forces derived from 4D-flow MRI and aneurysm wall permeability by DCE-MRI in a region-based analysis of unruptured saccular intracranial aneurysms (IAs). We performed 4D-flow MRI and DCE-MRI on patients with unruptured IAs of ≥ 5 mm to measure hemodynamic parameters, including wall shear stress (WSS), oscillatory shear index (OSI), WSS temporal (WSSGt) and spatial (WSSGs) gradient, and aneurysm wall permeability (K^{trans}) in different sectors of aneurysm wall defined by evenly distributed radial lines emitted from the aneurysm center. The spatial association between K^{trans} and hemodynamic parameters measured at the sector level was evaluated. Thirty-one patients were scanned. K^{trans} not only varied between aneurysms but also demonstrated spatial heterogeneity within an aneurysm. Among all 159 sectors, higher K^{trans} was associated with lower WSS, which was seen in both Spearman's correlation analysis (rho = − 0.18, $p = 0.025$) and linear regression analysis using generalized estimating equation to account for correlations between multiple sectors of the same aneurysm (regression coefficient = − 0.33, $p = 0.006$). Aneurysm wall permeability by DCE-MRI was shown to be spatially heterogenous in unruptured saccular IAs and associated with local WSS by 4D-flow MRI.

Keywords Intracranial aneurysm · Hemodynamics · 4D-flow · Permeability · Dynamic contrast-enhanced

Introduction

The pathophysiology of intracranial aneurysm (IA) rupture is not fully understood. Hemodynamic forces are thought to be implicated in the remodeling of aneurysm wall, which

Yajie Wang, Jie Sun, and Rui Li contributed equally.

✉ Ming Lv
dragontiger@163.com

✉ Huijun Chen
chenhj_cbir@mail.tsinghua.edu.cn

1 Center for Biomedical Imaging Research, Department of Biomedical Engineering, School of Medicine, Tsinghua University, Beijing, China

2 Department of Radiology, University of Washington, Seattle, WA, USA

3 Department of Interventional Neuroradiology, Beijing Neurosurgical Institute, Beijing Tiantan Hospital, Capital Medical University, Beijing, China

4 Key Laboratory of Imaging Diagnosis and Minimally Invasive Intervention Research, Clinical College of The Affiliated Central Hospital, Lishui University, Lishui, Zhejiang, China

5 School of Biomedical Engineering, ShanghaiTech University, Shanghai, China

6 Philips Healthcare, Beijing, China

7 Institute of Science and Technology for Brain-Inspired Intelligence, Fudan University, Shanghai, China

eventually results in rupture and subarachnoid hemorrhage. Most previous studies on the role of hemodynamics in IA are based on computational fluid dynamics (CFD) simulations without patient-specific flow measurements [1–3]. Associations of hemodynamic factors with pathological evidence of aneurysm wall remodeling have been described [1, 2], though existing data are limited to small surgical series with inherent challenges of radiology-pathology registration [1, 4]. Recent advances in four-dimensional (4D) flow MRI have allowed for comprehensive evaluation of hemodynamic parameters of IA [5, 6]. Furthermore, studies using dynamic contrast-enhanced (DCE) MRI have observed increased wall permeability in IAs at high risk of rupture [7, 8], suggesting that aneurysm wall permeability could serve as an in vivo marker of aneurysm wall remodeling and weakening.

The purpose of this study was to investigate the spatial association between hemodynamic forces derived from 4D-flow MRI and aneurysm wall permeability measured by DCE-MRI in a region-based analysis of unruptured saccular IAs.

Methods

This study was approved by the local Institutional Review Board, and all participants provided written informed consent. The data from this study are available from the corresponding author upon reasonable request.

Participants

Patients with unruptured saccular IA ≥ 5 mm in size, clinically diagnosed by DSA, CTA, or MRA, were referred to this IRB-approved study with informed consent. Small aneurysms (< 5 mm) were excluded in view of the limited spatial resolution of 4D flow MRI. Exclusion criteria included any contraindications to MR imaging or gadolinium contrast.

MRI protocol

Subjects were scanned at 3 T (Achieva TX or Ingenia CX, Philips Healthcare) using a 32-channel head coil. The aneurysm was first located by 3D time-of-flight (TOF). For subjects with multiple aneurysms, the largest aneurysm was selected as the index aneurysm. Then, 4D flow was acquired by a k-space segmented 3D radio-frequency-spoiled gradient-echo sequence [9] with peripheral pulse-gating and interleaved 3-directional velocity-encoding: TR/TE = 8.1/3.6 ms, flip angle = 20°, spatial resolution = 1 × 1 mm^2, slice thickness = 1 mm, slice coverage = 28 mm, temporal resolution = 45.84–75.76 ms, scan duration = 459–846 s, velocity encoding = 120 cm/s. Finally, DCE-MRI was acquired on the index aneurysm as pervious described [8]: TR/TE = 3.5 – 6.7/1.9 – 3.3 ms, flip angle = 15°, spatial resolution = 0.8 × 0.8 mm^2, slice thickness = 1–2 mm, slice coverage = 20 mm, temporal resolution = 10 s, scan duration = 6 min.

Image analysis

Figure 1 illustrates the image analysis workflow. DCE-MRI data were analyzed using the extended Kety/Tofts model [10] to generate K^{trans} maps. The slice with the K^{trans} hotspot (highest value) was chosen to draw two concentric ROIs surrounding the aneurysm: the first one was drawn just outside the aneurysm and the second one was drawn by expanding the first ROI 3 pixels outward.

In 4D flow analysis, hemodynamic parameters including total flow, peak flow, mean velocity, peak velocity, wall shear stress (WSS), oscillatory shear index (OSI), WSS temporal gradient (WSSGt), and WSS spatial gradient (WSSGs) were derived from the velocity field based on a validated quantitative analysis method combining B-spline interpolation and Green's theorem [11]. 4D flow images are isotropic. The slice corresponding to the DCE-MRI slice was generated, and the same ROI from DCE analysis was mapped to 4D flow for region-based measurements of WSS, OSI, WSSGt, and WSSGs.

Specifically, the circular ROI of each aneurysm was divided into sectors by evenly distributed radial lines emitted from the aneurysm center according to size: aneurysms of 5–10 mm were divided into 3 sectors; those of 10–20 mm were divided into 6 sectors; those of ≥ 20 mm were divided into 12 sectors.

Statistical analysis

Data were presented as count (percentage), mean ± standard deviation, or median (interquartile range). Spearman's correlation coefficient (rho) was used to evaluate any correlations between K^{trans} and hemodynamic parameters at the sector level. Associations between K^{trans} and hemodynamic parameters were evaluated in linear regression analysis using generalized estimating equation (GEE) to account for correlations between multiple sectors of the same aneurysm. Statistical analyses were performed using SPSS (Version 23.0. IBM Corp, Armonk, NY). p-values < 0.05 were considered statistically significant.

Results

Thirty-one patients were scanned. Clinical and imaging characteristics are summarized in the Supplemental Table I. Of the 31 aneurysms imaged, 20 (64.5%) were in the anterior circulation; the median size was 9.1 mm (7.2, 16.1); 2 (6.5%)

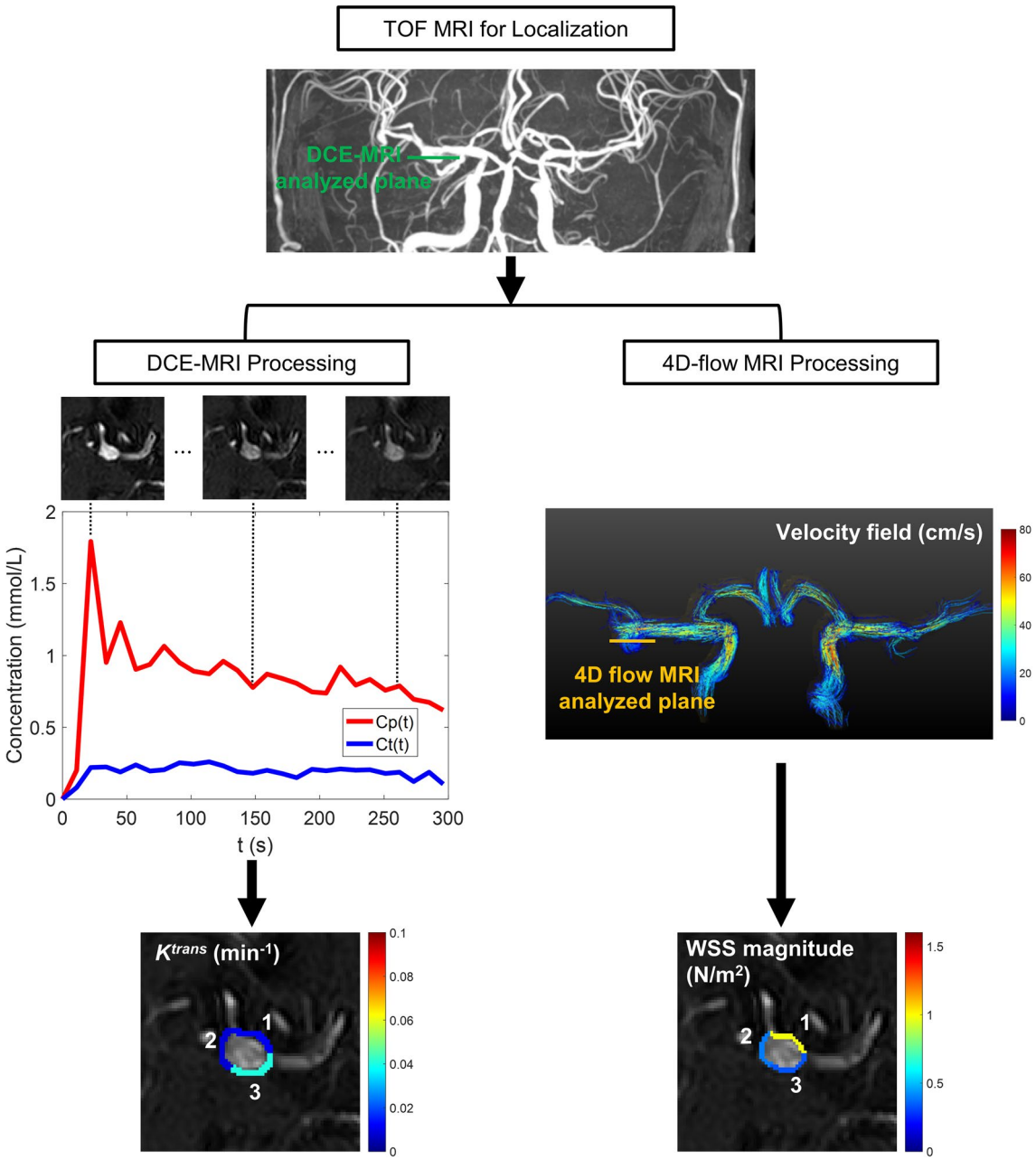

Fig. 1 Image analysis workflow and results of one aneurysm on the right middle cerebral artery. The aneurysm was localized using the TOF sequence. Arterial input function (AIF, Cp(t)) and contrast concentration in tissue adjacent to the aneurysm (Ct(t)) were derived from DCE-MRI images and were fitting to generate K^{trans} map. Hemodynamic parameters including wall shear stress (WSS) were derived from velocity field calculated from 4D-flow MRI data. The plane corresponding to the slice with the highest K^{trans} was analyzed. The circumference of the aneurysm was divided into 3 sectors anticlockwise. Sectors with higher K^{trans} showed relatively lower WSS magnitude

had blebs. K^{trans} not only varied substantially between aneurysms but also demonstrated spatial heterogeneity within an aneurysm (maximum K^{trans}: 0.0487 min^{-1} [0.0212, 0.103]; minimum K^{trans}: 0.0054 min^{-1} [0.0016, 0.0098]). Maximum K^{trans} correlated positively with aneurysm size (rho = 0.38, $p = 0.036$) while minimum K^{trans} did not ($p = 0.30$). Spatial heterogeneity within an aneurysm, measured as the coefficient of variation between different sectors, had a median of 85.9% (59.4, 104.0).

Among all 159 sectors, higher K^{trans} was associated with lower WSS, which was seen in both Spearman's correlation analysis (rho = − 0.18, $p = 0.025$) and GEE linear regression models (regression coefficient = − 0.33, $p = 0.006$) (Table 1). Although K^{trans} also correlated with temporal and spatial

Table 1 Association between K^{trans} and hemodynamic parameters in 159 sectors of 31 aneurysms

Hemodynamic parameters	Spearman's correlation		GEE linear regression*	
	Rho	*p* value	Coefficient	*p* value
WSS magnitude (N/m^2)	− 0.18	0.025	− 0.33	0.006
OSI (%)	− 0.09	0.24	0.22	0.15
WSSGt ($N/m^2/s$)	− 0.21	0.008	− 0.02	0.95
WSSGs (N/m^3)	− 0.20	0.012	− 0.30	0.23

WSS wall shear stress, *OSI* oscillatory shear index, *WSSGt* WSS temporal gradient, *WSSGs* WSS spatial gradient

*Right-skewed data were transformed to ranks before entering model

gradients of WSS in Spearman's correlation analysis, the spatial relationship with WSSGt or WSSGs was not seen in GEE linear regression after accounting for correlations between multiple sectors of the same aneurysm.

Discussion

The aneurysm wall is under constant influence from complex flow patterns, which is thought to be a major factor in driving pathological remodeling of aneurysm wall. However, specific hemodynamic conditions associated with aneurysm wall remodeling and rupture remain under debate. Because of the low incident of aneurysm rupture, most studies chose to cross-sectionally compare hemodynamic conditions between ruptured and unruptured aneurysms and yielded mixed results [12–15]. Biases cannot be excluded as the shape and hemodynamics of ruptured aneurysms may change after aneurysm rupture. Furthermore, the lack of patient-specific flow measurements and the assumptions of blood viscosity, vascular characteristics and boundary conditions in CFD modeling may affect comparisons between different patients though some studies sought to normalize hemodynamic parameters of aneurysm by those of the parent artery to alleviate this concern [12, 14]. This study used a surrogate marker of aneurysm wall degeneration, namely aneurysm wall permeability (K^{trans}), which can be measured locally in unruptured IAs, to evaluate potential impact of hemodynamic forces on aneurysm wall properties. Our region-based analysis revealed high spatial heterogeneity of aneurysm wall and that increased wall permeability colocalized with low WSS, which provided novel evidence that low WSS may induce aneurysm wall degeneration.

Due to technical constraints, only a few studies have examined the spatial heterogeneity of aneurysm wall and its relationship with hemodynamic conditions. The visual appearance of aneurysm wall under intraoperative microscopy has been used to identify atherosclerotic and super-thin regions though the classification scheme has not been histologically validated [1, 4]. Precise registration between in vivo imaging and intraoperative appearance is needed, representing a major challenge with this approach. Aneurysm wall enhancement (AWE) by vessel wall imaging presents a convenient marker for understanding the impact of hemodynamic forces on aneurysm wall. AWE regions have been associated with low WSS [16, 17]. However, a 7 T study recently showed that the association between WSS and AWE may depend on the location [18]. Both AWE by vessel wall imaging and aneurysm wall permeability by DCE-MRI remain to be histologically validated to understand the nature of these imaging markers. Particularly, AWE regions may encompass different histological characteristics (e.g., inflammation, atherosclerosis, thrombosis).

Despite the use of novel techniques in this study, a few limitations should be emphasized. With a growing footprint in neurovascular applications, 4D flow has been recently used to characterize flow patterns and hemodynamic forces in IA [6]. However, the limited spatial resolution of 4D flow restricts its application to relatively large IAs. We included only IAs of ≥ 5 mm (most would be at high risk) as the objective was not to test new markers for clinical decision-making but to understand pathophysiological relationships between focal hemodynamic forces and aneurysm wall remodeling. The results of this study should not be directly applied to small IAs (< 5 mm). The relationship between hemodynamic forces and wall permeability in small aneurysms still needs to be explored. The main limitation of the DCE-MRI protocol used in this study is that the acquired images are not isotropic. Subsequently, image analysis was limited to the acquired slices, which may not capture the wall region with the highest permeability. DCE-MRI protocols with isotropic resolution would be more ideal for IA characterization and should be a focus for future technical development.

Conclusion

In a region-based analysis of unruptured saccular intracranial aneurysms, aneurysm wall permeability by DCE-MRI was shown to be spatially heterogenous and associated with local WSS by 4D-flow MRI. By leveraging novel imaging techniques, our findings provide novel evidence that low WSS may induce aneurysm wall degeneration.

Supplementary Information The online version contains supplementary material available at https://doi.org/10.1007/s00415-021-10869-z.

Author contributions Study concept and design, all authors; acquisition of data, YW, RL, PL, JJ, CC, HQ, LZ, LJ, FP, MX, CK, SX, LH; analysis and interpretation of data, YW, JS, PL, XL, YC, HQ, YL, MF, YW, XW, QZ, ZC; drafting of the manuscript, YW, JS, HC; critical revision of the manuscript for important intellectual content, all

authors; statistical analysis, YW, JS; obtained funding, PL, AL, HC; study supervision, YL, ML, HC; responsible for the overall content as guarantor, ML, HC.

Funding This study was supported by the National Key Research & Development (R&D) Program of China (2017YFC0108702), the National Natural Science Foundation of China (81371540, 81771233, 81901197, and 81930119), the Beijing Municipal Natural Science Foundation (Z190024), and the Specific Research Projects for Capital Health Development (no. 2018-2-2041).

Data availability The data from this study are available from the corresponding author upon reasonable request.

Declarations

Conflicts of interest The authors declare that they have no conflict of interest.

Ethical approval This study was approved by the local Institutional Review Board.

Consent to participate All participants provided written informed consent.

References

1. Kadasi LM, Dent WC, Malek AM (2013) Colocalization of thin-walled dome regions with low hemodynamic wall shear stress in unruptured cerebral aneurysms. J Neurosurg 119:172–179. https://doi.org/10.3171/2013.2.jns12968
2. Cebral J, Ollikainen E, Chung BJ, Mut F, Sippola V, Jahromi BR, Tulamo R, Hernesniemi J, Niemelä M, Robertson A et al (2017) Flow conditions in the intracranial aneurysm lumen are associated with inflammation and degenerative changes of the aneurysm wall. Am J Neuroradiol 38:119–126. https://doi.org/10.3174/ajnr.A4951
3. Brinjikji W, Chung BJ, Jimenez C, Putman C, Kallmes DF, Cebral JR (2017) Hemodynamic differences between unstable and stable unruptured aneurysms independent of size and location: a pilot study. J Neurointerv Surg 9:376–380. https://doi.org/10.1136/neurintsurg-2016-012327
4. Cebral JR, Detmer F, Chung BJ, Choque-Velasquez J, Rezai B, Lehto H, Tulamo R, Hernesniemi J, Niemela M, Yu A et al (2019) Local hemodynamic conditions associated with focal changes in the intracranial aneurysm wall. AJNR Am J Neuroradiol 40:510–516. https://doi.org/10.3174/ajnr.A5970
5. van Ooij P, Potters WV, Guedon A, Schneiders JJ, Marquering HA, Majoie CB, vanBavel E, Nederveen AJ (2013) Wall shear stress estimated with phase contrast MRI in an in vitro and in vivo intracranial aneurysm. J Magn Reson Imaging JMRI 38:876–884. https://doi.org/10.1002/jmri.24051
6. Schnell S, Ansari SA, Vakil P, Wasielewski M, Carr ML, Hurley MC, Bendok BR, Batjer H, Carroll TJ, Carr J et al (2014) Three-dimensional hemodynamics in intracranial aneurysms: influence of size and morphology. J Magn Reson Imaging JMRI 39:120–131. https://doi.org/10.1002/jmri.24110
7. Vakil P, Ansari SA, Cantrell CG, Eddleman CS, Dehkordi FH, Vranic J, Hurley MC, Batjer HH, Bendok BR, Carroll TJ (2015) Quantifying intracranial aneurysm wall permeability for risk assessment using dynamic contrast-enhanced MRI: a pilot study. AJNR Am J Neuroradiol 36:953–959. https://doi.org/10.3174/ajnr.A4225
8. Qi H, Liu X, Liu P, Yuan W, Liu A, Jiang Y, Li Y, Sun J, Chen H (2019) Complementary roles of dynamic contrast-enhanced MR imaging and postcontrast vessel wall imaging in detecting high-risk intracranial aneurysms. Am J Neuroradiol 40:490–496. https://doi.org/10.3174/ajnr.A5983
9. Wetzel S, Meckel S, Frydrychowicz A, Bonati L, Radue EW, Scheffler K, Hennig J, Markl M (2007) In vivo assessment and visualization of intracranial arterial hemodynamics with flow-sensitized 4D MR imaging at 3T. AJNR Am J Neuroradiol 28:433–438
10. Tofts PS, Brix G, Buckley DL, Evelhoch JL, Henderson E, Knopp MV, Larsson HB, Lee TY, Mayr NA, Parker GJ et al (1999) Estimating kinetic parameters from dynamic contrast-enhanced T(1)-weighted MRI of a diffusable tracer: standardized quantities and symbols. J Magn Reson Imaging JMRI 10:223–232. https://doi.org/10.1002/(sici)1522-2586(199909)10:3%3c223::aid-jmri2%3e3.0.co;2-s
11. Stalder AF, Russe MF, Frydrychowicz A, Bock J, Hennig J, Markl M (2008) Quantitative 2D and 3D phase contrast MRI: optimized analysis of blood flow and vessel wall parameters. Magn Reson Med 60:1218–1231. https://doi.org/10.1002/mrm.21778
12. Xiang J, Natarajan SK, Tremmel M, Ma D, Mocco J, Hopkins LN, Siddiqui AH, Levy EI, Meng H (2011) Hemodynamic-morphologic discriminants for intracranial aneurysm rupture. Stroke 42:144–152. https://doi.org/10.1161/strokeaha.110.592923
13. Cebral JR, Mut F, Weir J, Putman CM (2011) Association of hemodynamic characteristics and cerebral aneurysm rupture. AJNR Am J Neuroradiol 32:264–270. https://doi.org/10.3174/ajnr.A2274
14. Miura Y, Ishida F, Umeda Y, Tanemura H, Suzuki H, Matsushima S, Shimosaka S, Taki W (2013) Low wall shear stress is independently associated with the rupture status of middle cerebral artery aneurysms. Stroke 44:519–521. https://doi.org/10.1161/strokeaha.112.675306
15. Zhou G, Zhu Y, Yin Y, Su M, Li M (2017) Association of wall shear stress with intracranial aneurysm rupture: systematic review and meta-analysis. Sci Rep. https://doi.org/10.1038/s41598-017-05886-w
16. Xiao W, Qi T, He S, Li Z, Ou S, Zhang G, Liu X, Huang Z, Liang F (2018) Low wall shear stress is associated with local aneurysm wall enhancement on high-resolution MR vessel wall imaging. AJNR Am J Neuroradiol 39:2082–2087. https://doi.org/10.3174/ajnr.A5806
17. Khan MO, Toro Arana V, Rubbert C, Cornelius JF, Fischer I, Bostelmann R, Mijderwijk HJ, Turowski B, Steiger HJ, May R et al (2020) Association between aneurysm hemodynamics and wall enhancement on 3D vessel wall MRI. J Neurosurg. https://doi.org/10.3171/2019.10.jns191251
18. Hadad S, Mut F, Chung BJ, Roa JA, Robertson AM, Hasan DM, Samaniego EA, Cebral JR (2021) Regional aneurysm wall enhancement is affected by local hemodynamics: a 7T MRI study. AJNR Am J Neuroradiol 42:464–470. https://doi.org/10.3174/ajnr.A6927